Supplementary Information

A. The Model Hamiltonian

Our model for hole transport through DNA is based upon a tight-binding ladder molecular Hamiltonian[31,33,34]. The model takes explicit account of the building blocks of the double strand DNA of type [5'-G(T)$_N$GGG-3']$^+$. Each nucleobase is regarded as a site with a local (on-site) ionization (hole) energy, ε_n, and with hole transfer integrals to nearest-neighbor sites (both intra-strand, $\alpha_{n,n+1}$, and inter-strand, β_n). The T and G nucleobases are numbered $n=1,...,N$ and $n=0,N+1,N+2,N+3$, respectively, and the complementary C and A nucleobases are numbered $n=N+5,...,2N+4$ and $n=N+4,2N+5,2N+6,2N+7$, respectively. The creation (annihilation) operator for a quasiparticle at the nth nucleobase site is denoted as $d_n^\dagger(d_n)$, and the Hamiltonian reads,

$$\begin{aligned}\hat{H}_{rigid} = &\sum_{n=0}^{N+3}\varepsilon_n d_n^\dagger d_n + \varepsilon_{N+4+n} d_{N+4+n}^\dagger d_{N+4+n} \\ &+\left\{\sum_{n=0}^{N+2}\alpha_{n,n+1} d_n^\dagger d_{n+1} + h.c.\right\} + \sum_{n=N+4}^{2N+6}\left\{\alpha_{n,n+1} d_n^\dagger d_{n+1} + h.c.\right\} \\ &+\sum_{n=0}^{N+3}\left\{\beta_n d_n^\dagger d_{N+4+n} + h.c.\right\}\end{aligned} \tag{0}$$

The Hamiltonian parameters are based upon the work by Voityuk et al[44-46] for the on-site hole energies and transfer integrals. Extended Data Table 1 summarizes the specific values used in our calculations.

In the calculations of local ionization potentials, each nucleobase is considered together with its two nearest neighbors, as they are π-stacked in a strand at the equilibrium geometry of the three dimensional helix. This parameterization does not account however, for the terminal nucleobases which have intra-molecular coupling only to a single neighboring nucleobase, and external coupling to the ex-molecular environment. It is therefore sensible to regard the terminal on-site energies as free parameters and study how changes in their values affect the charge transport kinetics. For each terminal nucleobase, the ionization potentials in the gas phase, I_{B^+}, and within the respective DNA trimer, I_{BBB^+} (as calculated in Ref. 44), provide physical bounds for the changes in the terminal on-site energy. In particular, the free nucleobase ionization potential is a lower bound for a C-terminal and an upper bound for a G-terminal, while the respective trimer ionization energies provide the complementary bounds.

Fig. S1 demonstrates that within the physically relevant interval, the on-site energies at the two C-terminal sites of sequences $[5'\text{-G(T)}_N\text{GGG-}3']^+$ hardly affect the transport kinetics.

The effect of the G terminal energy at the acceptor site (ε_{N+3}) is negligible for the longer DNA bridges (which are our prime interest in the present work), but for short bridges the effect is pronounced when $\varepsilon_{N+3} > 7.6eV$. Indeed, for the shorter bridges the CT kinetics is dominated by the downhill inelastic transitions, which require that the acceptor terminal site energy (ε_{N+3}) would be sufficiently lower than the donor energy. As ε_{N+3} approaches the donor on-site energy, ($\varepsilon_0 = 7.681\,eV$, see below) the back reaction becomes appreciable and the mechanism changes. For long bridges, transport is

facilitated by transitions to and from the bridge and the relative energies of the donor and acceptor terminals play a less critical role.

The effect of the G terminal energy at the donor site (ε_0) on the CT kinetics is significant also for longer bridges. At low values of ε_0 the transition from the sharp to the moderate drop of the rate with the bridge length depends on ε_0. At high values the effect is even more dramatic, as the transition between the two distinctive mechanisms becomes unclear. This behavior is due to the decrease in the energy gap between the donor and the bridge energy levels, which brings the donor from the off-resonant to the resonant transport regime. Since the precise value of the donor energy (within the bounds discussed above) depends not only on the DNA sequence, but also on the molecular environment, it is reasonable to regard it as a (single) fitting parameter of our model. The value $\varepsilon_0 = 7.681\, eV$ reproduces the transition between the two transport mechanisms at *N~4*, in accordance with the experimental investigation of Ref. 20.

B. The bath model

Fluctuations in the hole energy due to geometrical changes in the double helix structure and in the molecular environment are accounted for within the harmonic bath model,

$$\hat{H} = \hat{H}_{rigid} + \sum_j \hbar\omega_j (\mathrm{b}_j^{\dagger} b_j + \frac{1}{2}) + \sum_j \frac{\lambda_j}{\sqrt{2}} (\mathrm{b}_j^{\dagger} + b_j)\hat{P}_B \,, \qquad (2)$$

where $b_j^{\dagger}$ is the creation operator for a vibration quantum associated with the harmonic frequency ω_j . The coupling operator introduces correlation between fluctuations at different sites along the bridge. Considering the sequences, $[5'\text{-G(T)}_N\text{GGG-}3']^+$, the

operator $\hat{P}_B$ projects onto the A and T sites at the bridge. Using the above indexes, this reads, $\hat{P}_B = \sum_{n=1}^{N} (d_n^{\dagger} d_n + d_{n+N+4}^{\dagger} d_{n+N+4})$. According to this model, hole transport into any bridge site is associated with a displacement of the equilibrium positions of the (correlated) bath oscillators. The displacement is set by the microscopic coupling parameters $\{ \lambda_j \}$, which are derived from the bath spectral density. In this work a continuous model was assumed ($\lambda_j = \lambda(\hbar\omega_j) \to \lambda(\varepsilon)$), with an Ohmic spectral density[40],

$J(\varepsilon) \equiv 2\pi\lambda^2(\varepsilon)\rho(\varepsilon) = \frac{4\pi\eta}{\hbar\omega_c}\varepsilon e^{\frac{-\varepsilon}{\hbar\omega_c}}$ for $\varepsilon > 0$ and $J(\varepsilon) = 0$ otherwise. The parameter ω_c is the characteristic bath frequency which was set to $\hbar\omega_c = 0.1eV$, which implies that the spectral density covers the entire range of molecular and solvent vibrational frequencies, $0 < \hbar\omega \tilde{<} 0.5eV$. The parameter η defines the global reorganization energy of the bath modes in response to charge transfer into the bridge, $\eta = \int_0^{\infty} \frac{\lambda^2(\varepsilon)}{2\varepsilon}\rho(\varepsilon)d\varepsilon$, and measures the strength of coupling to the bath.

C. Reduced hole dynamics

Rewriting the full model Hamiltonian as follows, $\hat{H} = \hat{H}_{rigid} + \hat{H}_{nuc} + \hat{H}_{coup}$, with $\hat{H}_{nuc} \equiv \sum_j \hbar\omega_j (\mathrm{b}_j^{\dagger} b_j + \frac{1}{2})$, $\hat{H}_{coup} \equiv \sum_j \frac{\lambda_j}{\sqrt{2}} (\mathrm{b}_j^{\dagger} + b_j)\hat{P}_B$, it is convenient to follow the quasiparticle dynamics in a reduced space of the electronic degrees of freedom. Assuming that long range forces tend to stabilize the equilibrium structure, and to minimize external reorganization, we regard fluctuations around the equilibrium structure (deviations from the rigid structure) as a small perturbation. Following the Redfield

approach[65], the reduced quasiparticle dynamics can be represented in the basis of the eigenstates of $\hat{H}_{rigid}$ (see Eq. 1 and Table S1), defined by the equation, $\hat{H}_{rigid}|n\rangle = E_n|n\rangle$. The corresponding Markovian equation of motion for the reduced quasiparticle density operator, $\hat{\rho}(t)$, then reads,

$$\frac{d}{dt}\langle n'|\hat{\rho}(t)|n\rangle = \sum_{m,m'} R_{n',n,m,m'}\langle m|\hat{\rho}(t)|m'\rangle . \quad (3)$$

The elements of the Redfield propagator are given as follows,

$$\begin{aligned} R_{n',n,m,m'} &= -\frac{i}{\hbar}[E_{n'} - E_n]\delta_{n',m}\delta_{n,m'} \\ &+ \langle n'|\hat{\mathrm{P}}_B|m\rangle\langle m'|\hat{\mathrm{P}}_B|n\rangle\,\tilde{g}(E_{m'} - E_n) - \sum_k \langle m'|\hat{\mathrm{P}}_B|k\rangle\langle k|\hat{\mathrm{P}}_B|n\rangle\,\delta_{m,n'}\tilde{g}(E_{m'} - E_k) \quad (4) \\ &- \sum_k \langle n'|\hat{\mathrm{P}}_B|k\rangle\langle k|\hat{\mathrm{P}}_B|m\rangle\,\delta_{m',n} g(E_k - E_m) + \langle n'|\hat{\mathrm{P}}_B|m\rangle\langle m'|\hat{\mathrm{P}}_B|n\rangle\, g(E_{n'} - E_m) \end{aligned} ,$$

where, $g(\varepsilon) = \frac{1}{\hbar^2}\int_0^\infty d\tau C(\tau)e^{-\frac{i}{\hbar}\varepsilon\tau}$, $\tilde{g}(\varepsilon) = \frac{1}{\hbar^2}\int_0^\infty d\tau C^*(\tau)e^{-\frac{i}{\hbar}\varepsilon\tau}$, are Fourier transforms of the bath coupling correlation function, $C(\tau) = \sum_j \frac{\lambda_j^2}{2}[\frac{2}{e^{\frac{\hbar\omega_j}{KT}} - 1}\cos(\omega_j\tau) + e^{-i\omega_j\tau}]$. The bath thermal energy was taken to be, $K_B T = 0.025eV$, corresponding to room temperature. Eq. 3 can be further simplified when coherences between the quasiparticle eigenstates are negligible. For the DNA structures considered in this work the donor state population is dominated by a single eigenstate of $\hat{H}_{rigid}$, and therefore in the simulations the initial density operator corresponds to a pure eigenstate, $|n_D\rangle$, i.e., $\hat{\rho}(0) = |n_D\rangle\langle n_D|$, with zero populations at the other eigenstates and with zero coherences. Since weak coupling to the bath does not induce significant coherences on the time scale of the population transfer kinetics (as was verified numerically for particular cases considered here), one can

approximate, $\langle m|\hat{\rho}(t)|n\rangle \cong \langle m|\hat{\rho}(t)|n\rangle \delta_{m,n}$ at all times, and Eq. 3 yields the following equation for the eigenstates populations,

$$\frac{d}{dt}\langle n|\hat{\rho}(t)|n\rangle = \sum_{m\neq n} k_{n,m}\langle m|\hat{\rho}(t)|m\rangle - \sum_{m\neq n} k_{m,n}\langle n|\hat{\rho}(t)|n\rangle . \quad (5)$$

The respective state-to-state population transfer rates, $k_{n,m} \equiv |\langle n|\hat{\mathrm{P}}_B|m\rangle|^2 \, 2\,\mathrm{Re}[g(E_n - E_m)]$, can be divided into rates of energy absorption (when $E_n - E_m > 0$) or emission (when $E_m - E_n > 0$) from/to the bath, $k_{n,m} = k_{n,m}^{ab}$, or $k_{n,m} = k_{n,m}^{em}$, respectively, where

$$k_{n,m}^{em} = \frac{|\langle m|\hat{\mathrm{P}}_B|n\rangle|^2}{2\hbar} J(E_m - E_n) \frac{e^{\frac{E_m - E_n}{KT}}}{e^{\frac{E_m - E_n}{KT}} - 1}$$

$$k_{n,m}^{ab} = \frac{|\langle m|\hat{\mathrm{P}}_B|n\rangle|^2}{2\hbar} J(E_n - E_m) \frac{1}{e^{\frac{E_n - E_m}{KT}} - 1}$$

The obtained state-to-state rates turn out to be proportional to the square of the coupling matrix elements, $|\langle m|\hat{\mathrm{P}}_B|n\rangle|^2$, the bath spectral density, $J(E_m - E_n)$, and the thermal occupation number for absorption, $n(\omega) = \frac{1}{e^{\frac{\hbar\omega}{KT}} - 1}$, or emission, $n(\omega) + 1$.

D. Analytic formulation of Length-independent unfurling rates

The presence of delocalized quasiparticle eigenstates is necessary for the onset of the unfurling transport mechanism. Yet it is not sufficient in order to explain the length-independent long-range transfer rates as observed in our calculations for long DNA bridges at low temperatures (See the inset of Fig. 3 in the main text). As the bridge length increases, two competing phenomena are expected to affect the unfurling rates. On one

hand the density of quasiparticle eigenstates increases, which increases the number of transfer channels. On the other hand, per state, the probability amplitude at the contact sites to the donor (or to the acceptor) decreases, as the orbital spreads over increasingly longer bridges. A strictly length-independent transport rate implies that these two effects scale inversely with the number of bridge sites. In order to demonstrate such a scenario we consider a generic one dimensional tight binding model for a "donor-bridge" system.

$$H_{DB} = \varepsilon_D |0\rangle\langle 0| + t_0 |0\rangle\langle 1| + t_0 |1\rangle\langle 0| + \sum_{n=1}^{N} \varepsilon_B |n\rangle\langle n| + \sum_{n=2}^{N} t(|n\rangle\langle n-1| + |n-1\rangle\langle n|)$$

The model is characterized by the donor and bridge on-site energies, ε_D and ε_B, respectively, the inter-bridge transfer integral, t, and the donor-bridge transfer integral, t_0. Below we shall assume that as in the case of the studied DNA sequence ([5'-G(T)$_N$GGG-3']$^+$), the donor site energy is well separated from the bridge (off-resonant), i.e. $|t_0|, |t| << \varepsilon_B - \varepsilon_D$. The total transfer rate from the donor to the bridge is a sum over state-to-state rates, $k_{D\to B} = \sum_{l=1}^{N} k(\mathrm{E}_l - \mathrm{E}_g)$, where E_g is the ground state energy of H_{DB}, and $\{E_l\}$ are the excited states energies ($l = 1, 2, ..., N$). In the limit of large N the sum can be replaced by an integral,

$$k_{D\to B} \xrightarrow[N\to\infty]{} \int_{-\infty}^{\infty} k(\mathrm{E})\rho(E)\,\mathrm{dE},$$

where both $k(E)$ and the density of states, $\rho(E)$, depend on N. Let us consider a particular energy E within the spectrum of the bridge. For any N, the number of bridge

states up to the energy E can be approximated as $l(\mathrm{E}) \approx \frac{N+1}{\pi} arc\cos(\frac{E-E_B}{-2|t|})$, where we used the formula for the spectrum of the bridge Hamiltonian, $E_l = E_B - 2|t|\cos(\frac{\pi l}{N+1})$). The density of bridge states is therefore,

$$\rho(E) \equiv \frac{dl(E)}{dE} = (\frac{N+1}{\pi}) \frac{1}{\sqrt{4t^2 - (E-E_B)^2}},$$

which increases linearly with N. The respective rate, $k(\mathrm{E})$, depends on the coupling operator, i.e., $k(\mathrm{E}) \propto |\langle \psi_l | \hat{P}_B | \psi_g \rangle|^2$. In our model, $\hat{P}_B = \sum_{n=1}^{N} |n\rangle\langle n|$ is the projector to the bridge sites, $|\psi_g\rangle$ is the ground state function of H_{DB}, and $|\psi_l\rangle$ is the eigenstate closest in energy to the energy E. For $|t_0|, |t| << \varepsilon_B - \varepsilon_D$ we can regard $V = t_0|0\rangle\langle 1| + t_0|1\rangle\langle 0|$ as a small perturbation and calculate the matrix element using first order approximations for $|\psi_g\rangle$ and $|\psi_l\rangle$, which yields,

$$k(E) \cong \frac{t_0^2(\frac{2}{N+1})\sin^2(\frac{\pi l}{N+1})}{(E_B - E_D)^2} = (\frac{1}{N+1}) \frac{t_0^2/t^2}{2(E_B - E_D)^2} [4|t|^2 - (E_B - E)^2],$$

i.e., $k(E)$ decreases asymptotically as $1/N$. It therefore follows that in the limit of large N, $k(E)\rho(E) \propto \frac{t_0^2/t^2}{2\pi(E_B - E_D)^2} \sqrt{4t^2 - (E-E_B)^2}$, and therefore the transfer rate to the delocalized bridge states (the unfurling rate, $k_{D\to B}$) becomes length-independent.

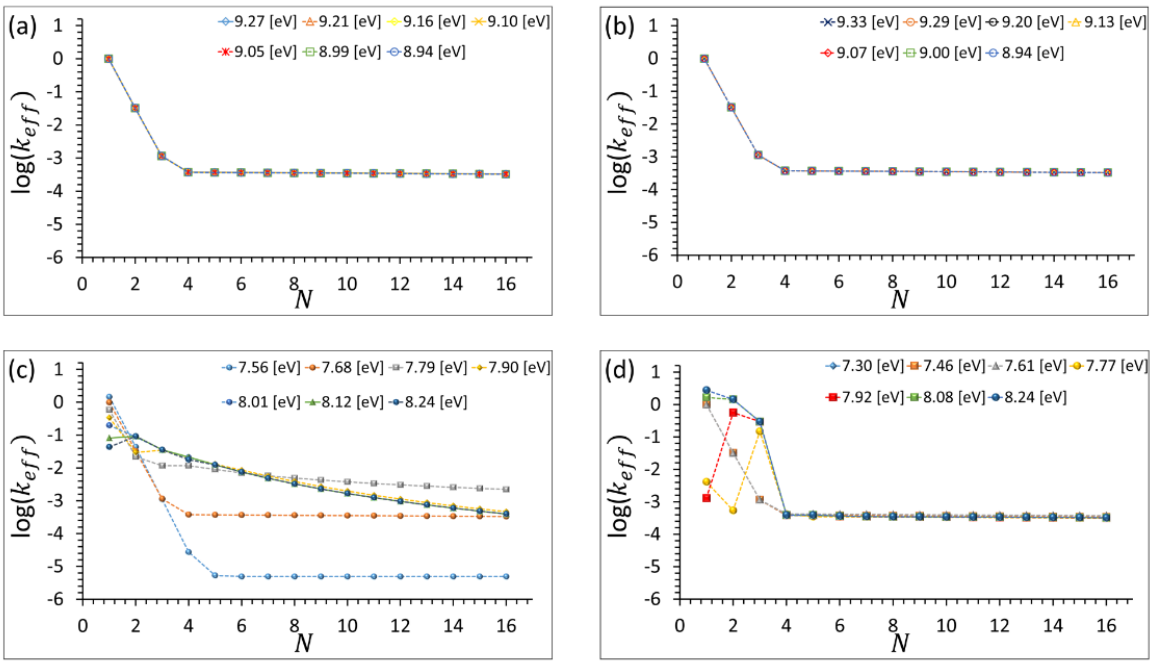

Figure S1

Figure S1: Effects of Terminal on-site Energies. Logarithm of the effective hole transport rate (nsec^{-1}) as a function of the bridge length for different terminal nucleobase site energies. (a) and (b) correspond to changes in the C terminal sites at the donor and acceptor moieties, respectively. (c) and (d) correspond to the complementary G terminal sites, respectively. In each plot a single terminal site energy is scanned within its physically relevant bounds, while all other model parameters are fixed to their values given in table S1. The bath model parameters are T=298 ^{o}K, $\hbar\omega_c = 0.1$ eV, $\eta = 0.007$.

On-site energies [eV]				Terminal on-site energies [eV]				
5'-AC$^+$C-3'	9.275	5'-CC$^+$A-3'	9.100	Site	C_{N+4}	C_{2N+7}	G_0	G_{N+3}
5'-AA$^+$C-3'	8.040	5'-CA$^+$A-3'	7.933		9.275	9.335	7.681	7.304
5'-GT$^+$T-3'	8.896	5'-TT$^+$G-3'	8.695	**Intra-strand coupling matrix elements [eV]**				
5'-GG$^+$T-3'	7.569	5'-TG$^+$G-3'	7.330	5'-AC-3'	0.061	5'-CA-3'	0.029	
5'-TT$^+$T-3'	8.952	5'-AA$^+$A-3'	7.806	5'-TG-3'	0.085	5'-GT-3'	0.137	
5'-GG$^+$G-3'	7.304	5'-CC$^+$C-3'	9.335	5'-GG-3'	0.084	5'-AA-3'	0.030	
5'-GT$^+$G-3'	8.587	5'-CA$^+$C-3'	8.073	5'-CC-3'	0.041	5-'TT-3'	0.158	
Inter-strand coupling matrix elements [eV]								
GC	0.05	AT	0.034					

Table S1

Table S1: Model Parameters. Electronic structure parameters for the double stranded DNA. On-site energies (calculated for DNA trimers of type $[XAY]^+$) are taken from Ref. 44. Intra-strand and inter-strand coupling are taken from Refs. 45, 46. Values for the terminal on-site energies were determined according to the analysis provided in this work.